

# The Effect of Nb Addition on the Microstructure and the High-Temperature Strength of Fe<sub>3</sub>Al Aluminide



PETR KRATOCHVÍL, MARTIN ŠVEC, ROBERT KRÁL, JOZEF VESELY,  
PAVEL LUKÁČ, and TOMÁŠ VLASÁK

The microstructural and high-temperature mechanical properties of Fe–26Al–*x*Nb (*x* = 3 and 5 at. pct) are compared. The alloys were investigated “as cast” and after hot rolling at 1473 K (1200 °C). Scanning electron microscopes equipped with EDS and EBSD were used for the microstructure and phase identification. The addition of 3 at. pct of Nb into the Fe<sub>3</sub>Al matrix leads to the formation of C14 λ—Laves phase (Fe,Al)<sub>2</sub>Nb (LP) particles spread in the Fe<sub>3</sub>Al matrix, while an eutectic with thin lamellae of LP C14 λ—Laves phase (Fe,Al)<sub>2</sub>Nb and matrix is also formed in the iron aluminide with 5 at. pct of Nb. The presence of incoherent precipitates is connected with the enhancement of the high-temperature strength and creep resistance.

<https://doi.org/10.1007/s11661-018-4524-4>

© The Minerals, Metals & Materials Society and ASM International 2018

## I. INTRODUCTION

IRON aluminides seem to be very promising materials for structural applications due to good properties of their high-temperature (HT) oxidation resistance and mechanical strength up to 873 K (600 °C), lower density in comparison to stainless steel (about 6.0 g/cm<sup>3</sup>), low raw material costs and savings of expensive alloy elements. These positive properties make Fe<sub>3</sub>Al intermetallic a candidate for replacing expensive high-alloyed stainless steels.<sup>[1–3]</sup> The improvement of HT mechanical properties (*e.g.*, yield strength, creep resistance, *etc.*) remains the aim of the research in the study of Fe<sub>3</sub>Al type iron aluminides. For the enhancement of these properties, alloying by proper elements is used<sup>[4,5]</sup>:

- solid solution hardening by elements with sufficient solubility in the Fe<sub>3</sub>Al matrix, *e.g.*, Cr, Mo or V
- Introducing a D0<sub>3</sub> order—*e.g.*, Ti increases the temperature of the D0<sub>3</sub>↔B2 transition,
- Coherent precipitates are the most effective way for enhancing the HT mechanical properties,

- Incoherent precipitates appear due to the limited solid solubility of some elements (*e.g.*, Zr, Nb or Ta).

The research task is to compare the effect of Nb with that of Zr recently tested.<sup>[6,7]</sup> The low Nb alloyed material was already tested by Kratochvil *et al.*<sup>[8]</sup> Alloying by Nb has a beneficial effect on the HT strength and creep resistance of Fe<sub>3</sub>Al type aluminides.<sup>[9–12]</sup> In alloys with 2 and 5 at. pct Nb,<sup>[9]</sup> a λ<sub>1</sub> Laves phase (C14) (Fe,Al)<sub>2</sub>Nb (LP) appears which is responsible for HT strengthening.

## II. EXPERIMENTAL

The alloys were prepared using vacuum induction melting and casting in 1. Brněnské strojírně, Velká Bíteš. The dimensions of the casts (40 × 30 × 80 to 90 mm<sup>3</sup>) were chosen for the preparation of the pieces for technological testing of these alloys in industry. Therefore, hot rolling (see below) was used to obtain the proper state of the material. The chemical composition of the investigated materials was determined by wet analysis and is given in Table I. The mean concentration of the technological impurities coming from the metals used for the preparation of the alloys was: 0.1 at. pct Cr, 0.01 at. pct B, 0.1 at. pct Mn and 0.06 at. pct C.

The surfaces of the alloys for the study of the microstructure and phase identification were prepared by standard metallographic methods and followed by mechanical-chemical polishing by OP-S suspension (Struers). The scanning electron microscopes (SEM) Tescan Vega SB and SEM Zeiss Ultra Plus were used to visualize the structure of the alloys. Both microscopes were equipped with an Oxford 20 mm<sup>2</sup> detector for an energy-dispersive X-ray analysis (EDX). The phase identification and type of crystal lattice

PETR KRATOCHVÍL, ROBERT KRÁL, JOZEF VESELY, PAVEL LUKÁČ are with the Department of Physics of Materials, Faculty of Mathematics and Physics, Charles University, Ke Karlovu 5, Prague 2, CZ-12116, Czech Republic. MARTIN ŠVEC is with the Department of Material Science, Faculty of Mechanical Engineering, Technical University of Liberec, Studentská 2, 460 01, Liberec, Czech Republic. Contact e-mail: martin.svec@tul.cz TOMÁŠ VLASÁK is with the Laboratory of High Temperature Materials, SVUM, a.s., Podnikatelská 565, 190 11, Prague 9, Czech Republic

Manuscript submitted October 10, 2017.

Article published online February 26, 2018

**Table I. The Nominal Chemical Composition of the Investigated Samples**

Sample	Chemical Composition [At. Pct]			
	Fe	Al	Nb	C (Impurity)
FA3Nb	bal.	25.8	2.7	0.05
FA5Nb	bal.	27.3	4.8	0.05

determination were performed by electron backscatter diffraction (EBSD) on an SEM Zeiss Ultra Plus equipped with an Oxford NodlysNano detector. The grain sizes were determined by EBSD (step size 6  $\mu\text{m}$ , HV 20 kV). The volume fractions of the observed phases were calculated by image analysis, the NIS – Elements from the SEM pictures taken in backscattered electrons (BSE). 10 SEM figures taken in different places in each sample was used for the computation of the volume fraction of the phases. The investigated area was  $1 \times 1 \text{ mm}^2$  for each figure. The individual values were averaged.

The dimensions of samples for the HT compression test were  $6 \times 6 \times 8 \text{ mm}^3$ . They were prepared by spark machining. Two types of samples were tested:

- The “as cast” samples
- The samples called “as received”, which were deformed by rolling at 1473 K (1200 °C) (a total reduction of 50 pct in four steps with a 15 pct thickness reduction for each pass).

Both types of samples were additionally annealed at 1273 K (1000 °C) for 50 hours to achieve phase equilibria and to annihilate internal stresses. This mentioned procedure did not change the structure of the LP, their configuration in the eutectic or volume fraction  $f_v$ . Subsequently polishing up to 1  $\mu\text{m}$  was the final step in the preparation of the samples for the HT compression tests.

The compression deformations were performed using an INSTRON 1186R at temperatures of 873 K, 973 K and 1073 K (600 °C, 700 °C, and 800 °C) with the initial strain rate of  $1.5 \times 10^{-4} \text{ s}^{-1}$ . The temperature was kept with the accuracy of 3 K. The characteristic parameter of the alloy in the present paper is the yield stress  $\sigma_{0.2}$ .

A creep test in tension in air were performed with samples machined (up to  $R_a = 1.6$ ) from the hot rolled alloys. Their gage length was 25, 5 mm diameter and with M12—threaded heads, and their axis was parallel to the rolling direction. After machining, the samples were additionally annealed at 1273 K (1000 °C) for 100 hours to remove all possible internal stresses and slowly cooled in the air. The tests were made with varying stresses to obtain the information about its influence on the creep rate (stress exponent). The testing temperatures were 873 K and 973 K (600 °C and 700 °C).

### III. EXPERIMENTAL RESULTS

#### A. Microstructure of the FA3Nb Alloy

The grains of the FA3Nb “as cast” alloy (Figure 1(a)) are large and have an irregular shape, their size is 200 to

500  $\mu\text{m}$ . The precipitates are  $\lambda_1$  Laves phase (C14) (Fe, Al)<sub>2</sub>Nb. These appear as smaller irregular shapes up to 10  $\mu\text{m}$  and as needle—like up to 50  $\mu\text{m}$  long (Figure 1(b)). The following composition of precipitates was determined (at. pct): (52.7  $\pm$  0.2) Fe, (19.6  $\pm$  0.6) Al and (27.7  $\pm$  0.1) Nb. They are homogeneously distributed both along the grain boundaries (marked by arrows in Figure 1(b)) and inside the grains.

Hot—rolling makes the LP particles in the FA3Nb “as received” sample finer and homogeneously distributed, see Figure 2. The appearance of the needle like precipitates of LP is smaller.

#### B. Microstructure of the FA5Nb Alloy

The grains of the FA5Nb “as cast” alloy are coarse (Figure 3(a)). The LP (C14) forms a eutectic with the Fe<sub>3</sub>Al matrix (Figure 3(b)). The composition of the LP is (at. pct): (56.4  $\pm$  0.8) Fe, (18.5  $\pm$  1.6) Al and (25.1  $\pm$  1.1) Nb. The LP forms 40 pct of the fraction volume of the eutectic. This is connected with the solubility of the Nb in the aluminide lattice. Similar to the “as cast” iron aluminides alloyed with Zr, a well-developed eutectic already appears in the alloy with 2 at. pct Zr<sup>[6,7]</sup> due to the lower solubility of the Zr in the iron aluminide lattice.

Also, only two other phases have been very rarely observed in the FA5Nb: niobium carbides NbC (detailed in Figure 3(b), marked as “A”) with a trigonal lattice and metastable  $\mu$ —phase Nb<sub>19</sub>(Fe<sub>1-x</sub>Al<sub>x</sub>)<sub>21</sub> (detailed in Figure 3(b), marked as “B”).

Hot rolling (the FA5Nb “as received”) results in the distortion of the primary eutectic structure in a dense configuration of the isolated LP particles in the matrix, see Figure 4. They are homogeneously distributed and aligned parallel to the rolling direction.

#### C. The Yield Strength at HT

The values of the HT yield strength  $\sigma_{0.2}$  are proportional to the volume fractions  $f_v$  of the LP (inclusive of the data for iron aluminide with 1 at. pct of Nb<sup>[8]</sup>). The values of  $f_v$  are given in Table II, the  $f_v$  of the LP increases with the increasing concentration of the Nb. The HT compression yield strengths  $\sigma_{0.2}$  are given for the “as cast” in Figure 5(a) and for the “as received” (rolled at 1473 K (1200 °C)) in Figure 5(b) and summarized in Table III also.

The values of the yield strength  $\sigma_{0.2}$  of the FA3Nb and FA5Nb “as received” alloys are higher than those for the “as cast” alloys for all temperatures. The values of yield strength  $\sigma_{0.2}$  of the “as cast” alloys are

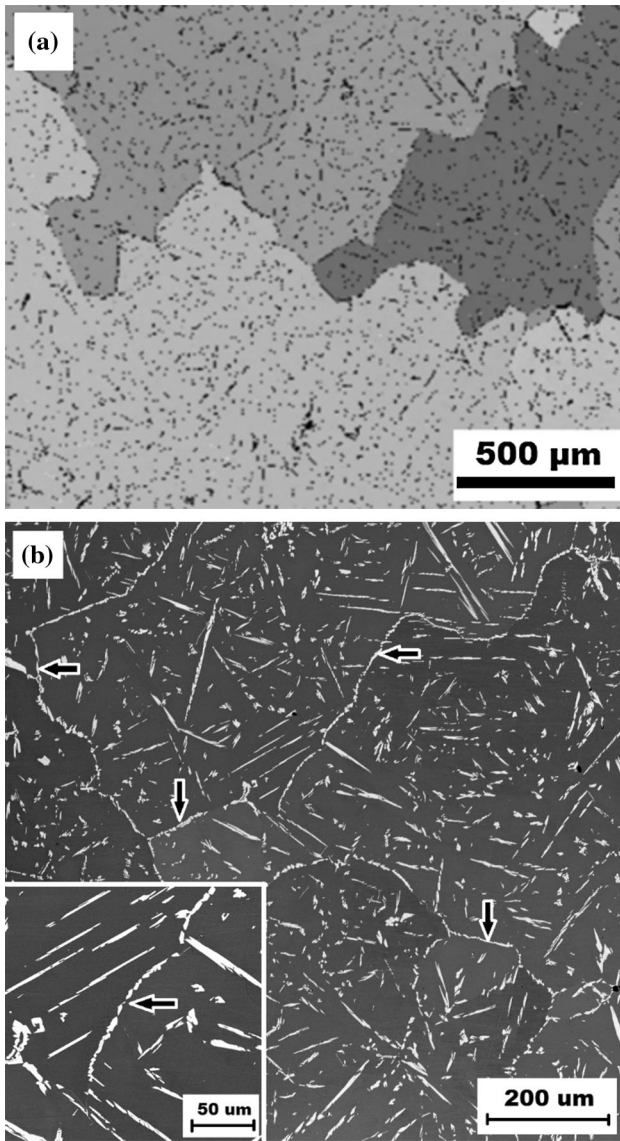


Fig. 1—The structure of the FA3Nb “as cast” sample: (a) the grains of the FA3Nb (EBSD) – the different shading color indicates differences in the crystal lattice orientation inside the matrix, (b) distribution of the LP (BSE detector); Gray: Fe<sub>3</sub>Al matrix, white: λ—LP.

increasing for all temperatures with an increasing niobium content and decreasing with an increasing temperature. The values of the HT  $\sigma_{0.2}$  yield stress for the corresponding material alloyed by Zr (marked 25\_5)<sup>[6]</sup> are added into Figure 5(a) for comparison. The following is surprisingly not valid for the “as received” alloys: The strength  $\sigma_{0.2}$  of the FA5Nb is lower than that of the FA3Nb (with the exclusion of the values at 873 K (600 °C)). For a comparison, the results obtained for the FA1Nb “as received” alloy<sup>[8]</sup> are added into Tables II and III and to Figure 5(b). The values of the yield strength  $\sigma_{0.2}$  of this alloy are, at all testing temperatures, lower than those for the FA3Nb and FA5Nb alloys.

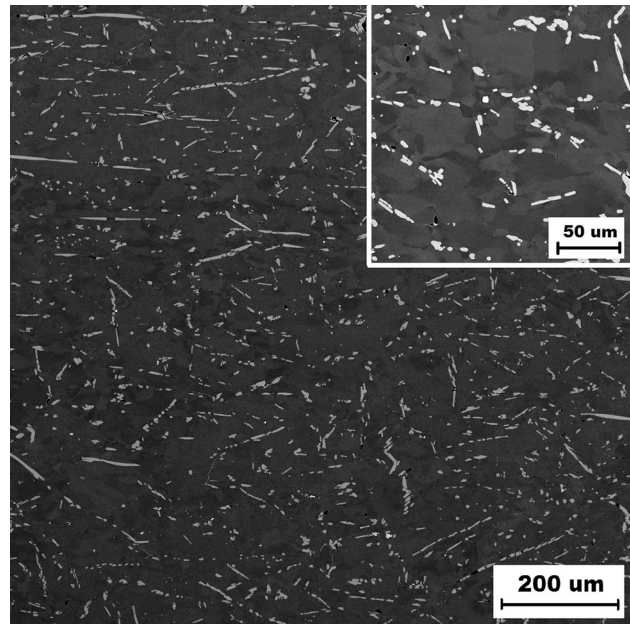


Fig. 2—The microstructure of the FA3Nb “as received” sample (BSE detector); Dark gray: Fe<sub>3</sub>Al matrix, light gray/white: λ—LP.

#### D. Creep

Creep strength is very important for high-temperature structural application. Therefore, the creep behavior of the studied materials was tested. The stress dependences of the creep rate  $\dot{\epsilon}$  of the FA3Nb and FA5Nb “as received” alloys at 873 K and 973 K (600 °C and 700 °C) are shown in Figure 6. The steady state creep rate may be expressed by an empirical equation in the following form:

$$\dot{\epsilon} = A \times \left(\frac{\sigma}{\mu}\right)^n \times \exp\left(\frac{Q}{R \times T}\right), \quad [1]$$

where A is the material constant and  $\sigma$  is the applied stress,  $\mu$  is the shear modulus,  $n$  the stress exponent,  $Q$  the activation energy,  $R$  is the gas constant and  $T$  is the absolute temperature.<sup>[14]</sup> The values of the stress exponent are given in Table IV.

## IV. DISCUSSION

First of all, it must be mentioned that the configuration of the LP in both “as cast”—alloys is substantially different: In the “as cast” alloys, the arrangements of LP act as obstacles for the dislocation movement. These are both (i) the individual particles distributed in the matrix (FA3Nb and FA5Nb) and (ii) the continuous barriers of eutectic formed by the Laves phase and the matrix (FA5Nb). One can imagine that the barriers of the eutectic make an efficient obstacle for the movement of the dislocations during the HT deformation. Such a case was described by Kejzlar *et al.*<sup>[6]</sup> with a similar additive—Zr. Eutectic regions were formed there with 2 at. pct of Zr already and the authors related the HT mechanical properties to the fraction volume of the



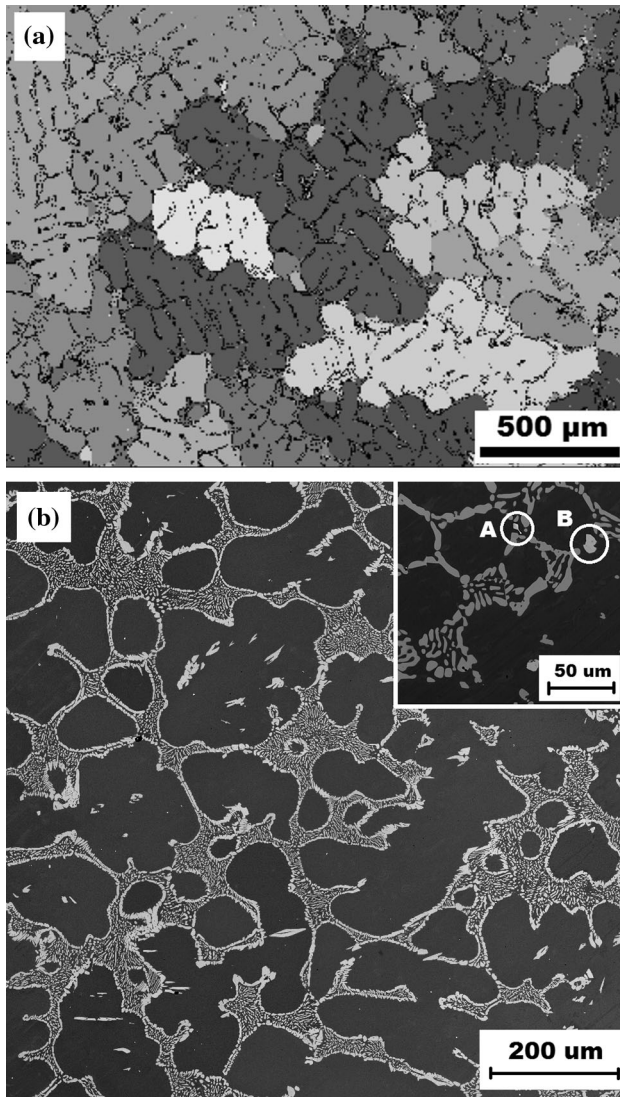


Fig. 3—The structure of the FA5Nb “as cast” sample: (a) the grains of the FA5Nb (EBSD), (b) distribution of the LP (BSE detector); Gray: Fe<sub>3</sub>Al matrix, white: λ—LP.

eutectic, which already appeared in this alloy at a lower concentration of the additive due to the lower solubility of Zr<sup>[13]</sup> in the iron aluminide compared to that of the Nb.<sup>[12]</sup>

We suppose that the strength of the “as cast” alloys is determined by the fraction volume of the eutectic in the respective alloy. Using the data in Table II, the  $f_v$  of the eutectic in the alloy FA5Nb “as cast” is 23 pct plus the excluding LP, which is not part of eutectic. This is greater than the  $f_v$  of the individual LP particles which can be taken as the only strengthening mechanism in the FA3Nb “as cast”. The values of the HT yield strength of the Fe<sub>3</sub>Al with 5 at. pct of Zr material<sup>[6]</sup> with an  $f_v$  equal to 47.6 pct of the eutectic are added into Figure 5(a). The HT  $\sigma_{0.2}$  yield strength is increasing with an

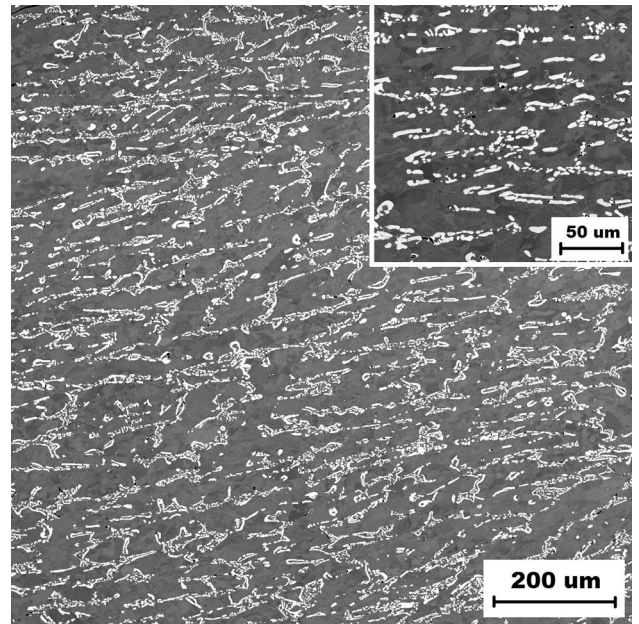


Fig. 4—The structure of the FA5Nb “as received” sample (BSE detector); Gray: Fe<sub>3</sub>Al matrix, white: λ—LP.

Table II. Volume Fraction of the LP in the Investigated Samples

Sample	The $f_v$ of the Eutectic	
	The $f_v$ of the LP [Pct]	(LP + Matrix) [Pct]
FA1Nb hot rolled <sup>[8]</sup>	1.3	—
FA3Nb as cast	8.1	—
FA3Nb hot rolled	8.2	—
FA5Nb as cast	3.5*	9.2 + 13.8
FA5Nb hot rolled	15.6	—

\*Not being part of the eutectic.

increasing fraction volume of the LP (in both the Nb and the Zr alloyed Fe<sub>3</sub>Al also). In spite of the fact that the concentrations of Al in both cases—alloys with Nb and Zr slightly differ (27.3 in this paper compared to 25.4 in<sup>[6]</sup>), the influence of Al on Fe<sub>3</sub>Al on the strength at a HT is very small.<sup>[1]</sup>

The situation is different in the material denoted “as received”: After rolling at 1473 K (1200 °C) the eutectic configuration in the FA5Nb alloy is damaged and a homogeneous distribution of separated LP particles in the matrix is generated. Thus, the continuous eutectic barrier for the movement of the dislocations in the “as cast” alloy is substituted by the individual LP particles spread in the matrix. The configuration enhances the strength (see Table III) at 873 K (600 °C) and 973 K (700 °C), but eliminates the hardening effect at 1073 K (800 °C).

The situation is completely different in the FA3Nb alloy in which the rolling makes the distribution of the LP even denser and the particles themselves smaller, which makes the alloy even harder at 1073 K (800 °C).

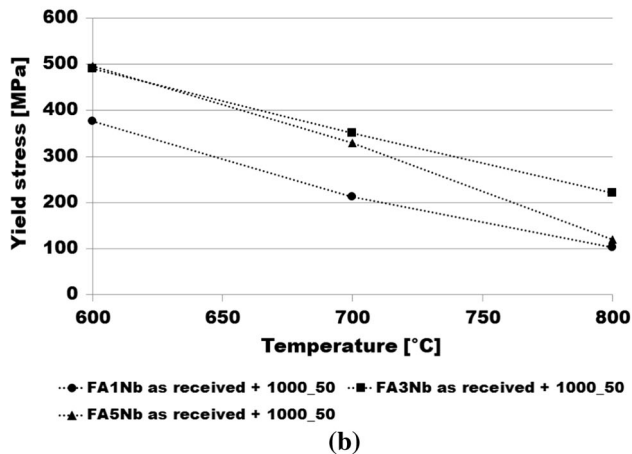
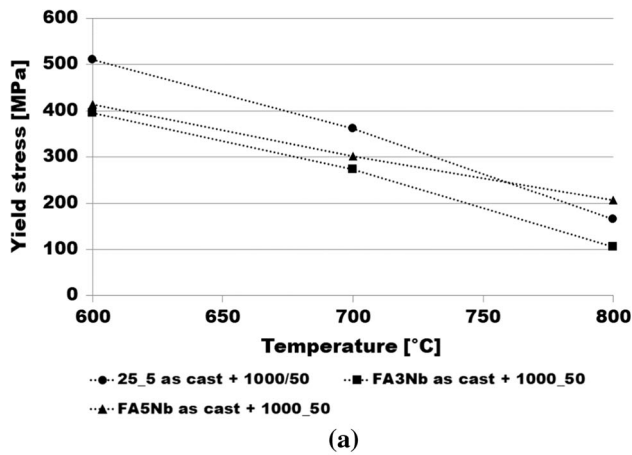


Fig. 5—Comparison of the HT yield stress curves for (a) the “as cast” samples, (b) the rolled samples (“as received”).

Table III. The Compression Yield Stress  $\sigma_{0.2}$  [MPa] of the “As Cast”/Rolled Samples

Sample	Temperature [K/°C]		
	873/600	973/700	1073/800
FA1Nb <sup>[8]</sup>	−/377	−/213	−/103
FA3Nb	396/490	274/351	106/221
FA5Nb	414/496	302/329	207/120

The value of the stress exponent determined from the stress dependence of the creep rate is important for estimating creep mechanisms. A stress exponent of five suggests that the creep rate is controlled by the climb of the dislocations over the particles.<sup>[14,15]</sup>

In the case of the FA3Nb samples crept at 973 K (700 °C), the value of  $n$  is close to 1 which suggests the activity of a bulk diffusion mechanism. It should be mentioned that for low applied stresses and high temperatures, the creep rate may be expressed as.<sup>[16,17]</sup>

$$\dot{\varepsilon} = A_D \cdot \frac{\sigma}{k \cdot T}, \quad [2]$$

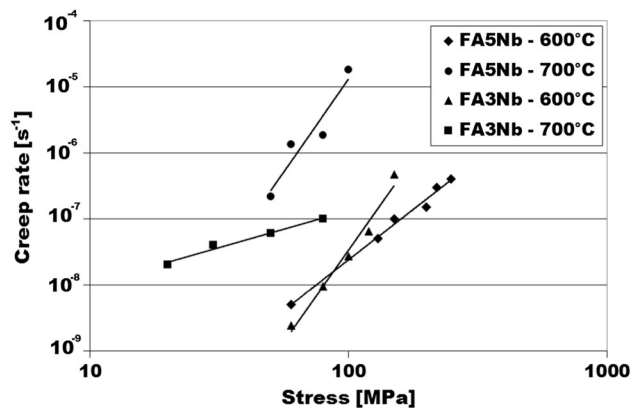


Fig. 6—Dependence of the creep rate on the stress of the FA3Nb and FA5Nb “as received” alloys.

Table IV. Stress Exponents  $n$  in Creep Experiments

Sample	Temperature [K/°C]	
	973/700	873/600
FA5Nb	5.6	3.0
FA3Nb	1.2	5.5

where  $A_D$  depends on the atomic volume  $\Omega$ , the grain size  $d$  and on the bulk diffusion coefficient  $D_L$ .

## V. CONCLUSIONS

- The eutectic arrangement of LP + Fe<sub>3</sub>Al forms in the “as cast” alloy with higher Nb content (Fe<sub>3</sub>Al with 5 at. pct Nb—FA5Nb). This arrangement is responsible for the increase of the  $\sigma_{0.2}$  yield stress at HTs.
- The eutectic configuration in FA5Nb is damaged after hot rolling and the homogeneous distribution of Laves phase particles is formed. This enhances the HT yield stress.
- In the “as cast” Fe<sub>3</sub>Al with 3 at. pct Nb (FA3Nb), the low density configuration of Laves phase particles appear. The increase of the HT yield strength is smaller than in the case of the alloy with a higher content of Nb.
- The creep stress exponent  $n \approx 5$  [FA5Nb and FA3Nb at 873 K (600 °C)] suggests that the creep rate is controlled by the climb of the dislocations over the particles,  $n$  is close to 1 for the FA3Nb sample crept at 973 K (700 °C) which suggests the activity of a bulk diffusion mechanism.

## ACKNOWLEDGMENTS

The research was supported by the Grant Agency of the Czech Republic through the Project No. 16-05608S and with the support of the Institutional

Endowment for the Long Term Conceptual Development of Research Institutes (at the Technical University of Liberec), as provided by the Ministry of Education, Youth and Sports of the Czech Republic in the year 2017.

## REFERENCES

1. C.G. McKamey: *Physical Metallurgy and Processing of Intermetallic Compounds*, Springer, Boston, 1994, pp. 351–91.
2. N.S. Stoloff: *Mater. Sci. Eng. A.*, 1998, vol. 258, pp. 1–14.
3. S.C. Deevi and V.K. Sikka: *Intermetallics*, 1996, vol. 4, pp. 357–75.
4. M. Palm: *Intermetallics*, 2005, vol. 13, pp. 1286–95.
5. M. Palm, A. Schneider, F. Stein, and G. Sauthoff: *Mater. Res. Soc. Symp. Proc.*, Vol. 842, 2005, S1.7.1–S1.7.12.
6. P. Kejzlar, P. Kratochvíl, R. Král, and V. Vodičková: *Metall. Mater. Trans. A.*, 2014, vol. 45A, pp. 335–42.
7. P. Kratochvíl, P. Kejzlar, R. Král, and V. Vodičková: *Intermetallics*, 2012, vol. 20, pp. 39–46.
8. P. Kratochvíl, M. Švec, and V. Vodičková: *Metall. Mater. Trans. A*, 2017, vol. 48, pp. 4093–96.
9. O. Prymak and F. Stein: *Intermetallics*, 2010, vol. 18, pp. 1322–26.
10. D.G. Morris and M.A. Muñoz-Morris: *Intermetallics.*, 2012, vol. 23, pp. 169–76.
11. D.M. Dimiduk, M.G. Mendiratta, D. Banerjee, and H.A. Lipsitt: *Acta Metall.*, 1988, vol. 36, pp. 2947–58.
12. M. Palm: *J. Alloys Compd.*, 2009, vol. 475 (1–2), pp. 173–77.
13. V. Raghavan: *J. Phase Equilib. Diffus.*, 2006, vol. 27, pp. 284–87.
14. J. Čadek: *Creep in Metallic Materials*, Academia, Prague, 1988.
15. O.D. Sherby and J. Wertman: *Acta Metall.*, 1979, vol. 27, pp. 387–400.
16. C. Herring: *J. Appl. Phys.*, 1950, vol. 21, p. 437.
17. F. R. N. Nabarro: Reports on Conference on Strength of Solids, The Physical Society, London, 1948, pp. 75.